Reports on Geodesy and Geoinformatics, 2023, Vol. 116, pp. 1–8

DOI: 10.2478/rgg-2023-0005
Received: 24 April 2023 / Accepted: 3 July 2023
Published online: 4 August 2023

ORIGINAL ARTICLE

Methodology for the measurement and 3D modelling of cultural heritage: a case study of the Monument to the Polish Diaspora Bond with the Homeland

Czesław Suchocki [1*], Sebastian Okrój and Wioleta Błaszczak-Bąk [2]

[1]Faculty of Civil Engineering, Environmental and Geodetic Sciences, Koszalin University of Technology, Śniadeckich 2, 75-453 Koszalin, Poland
[2]Faculty of Geoengineering, University of Warmia and Mazury in Olsztyn, Oczapowskiego 1, 10-719 Olsztyn, Poland

*czeslaw.suchocki@tu.koszalin.pl

Abstract

The documentation of cultural heritage objects requires a special approach, as does the collection of materials describing a monument over a period of time. With the development of measurement and information technologies, such documentation can be supplemented by a digital model of the object, a 3D visualization in a computer environment, or a miniature, scaled 3D printout. This paper presents a methodology for developing the 3D documentation of the Monument to the Polish Diaspora Bond with the Homeland, a sculpture located in Koszalin, Poland. In the study, terrestrial laser scanning supplemented with photos was used for non-invasive measurements, and existing free software was used to generate a 3D model. The results of the study can supplement the technical documentation of an object so as to preserve its characteristic features and ease the conservation of monuments. The proposed approach to modelling 3D monuments can be used to create HBIM documentation.

Key words: terrestrial laser scanner, sculpture, cultural heritage documentation, remote sensing, HBIM

1 Introduction

Three-dimensional modelling of architectural structures for monitoring, conservation, and restoration alterations in cultural heritage objects has special challenges for data acquisition and processing. In many cases, because of the complexity of the structures, 3D modelling can be time-consuming and may include some difficulties. Laser scanning technology, due to its accuracy, speed, and flexibility, is a reliable and advantageous technology for the reconstruction and conservation of monuments. Laser scanning can be used for the 3D documentation of cultural heritage for the future (Nowak et al., 2020; Temizer et al., 2013). Most often, terrestrial laser scanning (TLS), unmanned aerial vehicle laser scanning, or mobile laser scanning are used for this purpose (Klapa and Gawronek, 2022; Rodríguez-Gonzálvez et al., 2017; Xu et al., 2014; Yan et al., 2010). TLS is a very efficient data collecting tool and it was the first remote and non-invasive surveying technique. However, for hard-to-reach places or to increase the detail of measurements in characteristic places of an object, laser scanning can be performed using smartphones or a tablet with a LiDAR sensor (Murtiyoso et al., 2021; Shih and Chen, 2020; Teppati Losè et al., 2022). In addition to laser scanning, technologies based on a series of photos taken, which, after processing, create a 3D model, can be used (Bocheńska et al., 2019; Kadhim et al., 2023). Conventional approaches to building 3D models typically rely on detecting, matching, and triangulating local image features (e.g., patches, superpixels, edges, and SIFT features) (Zheng et al., 2020). Another technique of data acquisition used to record the geometry of historical monuments in the form of a textured 3D point cloud is structure from motion (SfM) photogrammetry (Al Khalil, 2020).

Selecting the method for obtaining data about an object depends primarily on the object's size, structure, and accessibility. Monuments located in the field without curtains (such as bushes) that are quite high and have complex shapes are best measured using TLS. More data about cultural heritage objects are obtained in order to build historic building information modelling (HBIM). HBIM is

a technology that documents and analyses 3D model information for reverse engineering using laser scan and image survey data for buildings with heritage value (Sammartano et al., 2023; Youn et al., 2021). TLS point cloud can be a source of data for analysing the condition of the structure of a historic building and examining the verticality of the elements, the shape, and the structure of existing deformations. Interpretation of the intensity of a laser beam reflection allows for research on the condition of a structure and the type and degree of wear of the materials from which a monument was made. The sensitivity of this parameter to the colour, roughness, and humidity of a scanned surface allows for in-depth analyses, including, for example, detecting moisture (Suchocki et al., 2020b; Tan et al., 2016). Additional information about the type of materials is also provided by the texture seen in photos. The mapping of the point cloud in the RGB colour space facilitates the data interpretation and visual assessment of the material's condition in terms of damage. The high resolution of an obtained point cloud allows for the precise detection of existing cavities and cracks and assessment of their sizes (Suchocki et al., 2020a, 2021). After modelling measured losses, it is possible to calculate their volumes, measure the widths of the cracks, and determine their internal structures. Therefore, the process of conducting 3D modelling of an object is important not only for the reconstruction of the object and creating documentation, but also for the purposes of analysing and maintaining the monument. Modelling methods must take into account the complexity of a monument that arises from its shape and architectural elements and the number of these elements required to create a given monument (Mistretta et al., 2019). A properly prepared model can be 3D-printed for presentation purposes (Neumüller et al., 2014; Wabiński and Mościcka, 2019). It should be noted that the virtual representation of heritage and the production of 3D printouts are very useful and make the process highly interactive. Three-dimensional printing technology is constantly being developed and is becoming more accessible and cheaper.

This paper presents the TLS measurement procedure and related data processing for the purpose of inventorying a historic sculpture in the context of preparing a 3D model for visualisation in software and 3D printing. In order to improve the final quality of realistic visualisation of the 3D digital model on a monitor built from TLS data, the RGB data for texturing was taken with an external high-resolution digital camera. Typically, researchers use commercial software for such data processing. Using open-source software allows for cost-free data post-processing. The main aim of this research was a case study of the documentation of the Monument to the Polish Diaspora Bond with the Homeland using TLS technology and free software.

2 Research methodology

A methodology for obtaining and processing data from TLS measurements was proposed in order to build a 3D sculpture model. The 3D model can be used to create a faithful copy of a sculpture using 3D printing technology. The methodology consists of a sequence of stages according to the scheme shown in Figure 1.

Stage 1 (data acquisition) deals with measurement planning and depends on the tested sculpture and the TLS used. It should be noted that two different types of TLS can be used in monument documentation: time-of-flight (TOF) scanners and phase-shift (PS) scanners (Guidi, 2014). These scanners are typically characterized by different speeds of data acquisition, measurement ranges, and accuracy of distance measurement. TOF scanners have a larger measurement range but acquire data over a longer time with lower accuracy compared to PS scanners. Scan resolution is one of the most important parameters and should be adjusted according to the complexity of the sculpture. For sculptures with small details, the scanning resolution should be increased, but it's important to remember that this will also increase the measurement time.

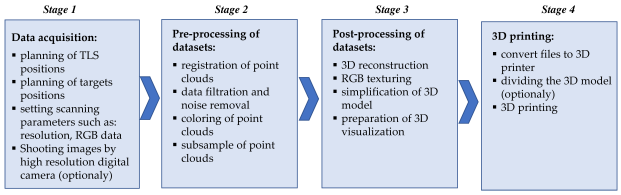

Figure 1. The main stages of the proposed methodology

The minimum number of scanning positions should be defined to ensure full coverage of the inventoried sculpture. Typically, four measuring stations are sufficient. Increasing the number of scanning positions can provide useful information, but it can also result in the redundancy of the point clouds. In addition, an optimum distance between the scanner and the sculpture should be chosen. Some scanner manufacturers additionally equip TLS equipment with a telescope tripod, which allows for scanning at heights of up to 4.50 m (see Appendix A). This option is very useful for measuring tall sculptures at close range or taking measurements of the top of a sculpture. During the measurements, it is necessary to decide how the point clouds will be registered in one coordinate system in the pre-processing stage. Cloud-to-cloud and plane-to-plane methods are the typically used approaches, and they can additionally be used where special artificial targets are the common points of the point clouds in the registration process (Cheng et al., 2018; Favre et al., 2021).

When obtaining data for 3D modelling purposes, setting the appropriate scanning resolution is a key element. The scanning resolution should depend on the detail and diversity of the sculpture's surface. It should be noted that an increase in the scanning resolution may result in data redundancy and increase the scanning time. In addition, the scanner can acquire RGB data using a built-in digital camera. In order to improve the quality of the RGB data, a sequence of photos can optionally be taken with an external high-resolution digital camera. Because of this, realistic and very good quality texturing of the 3D model can be performed during the post-processing stage.

Stage 2 (pre-processing of the datasets) includes the registration of the point clouds in one coordinate system, point cloud filtration from noise, generation of colour point clouds based on the RGB images taken using TLS, and down-sampling the datasets. Registration of the point clouds is usually completed automatically or semi-automatically using dedicated software. Point cloud filtering removes irrelevant and outlier observations based on various methods including a range filter, an intensity filter, a single-pixel filter, a thin filter (Hui et al., 2019). The available data-filtering methods depend on the software used, and this process is usually fully automated. Very often, point clouds at too high a resolution or overlapping neighbouring point clouds will cause redundancy in the dataset of a monument's surfaces. Datasets that are too large may hinder the post-processing stage. In this case, down-sampling the point clouds is needed to optimize the dataset. Various approaches are known, such as the random method, the space method, the octree method, the curvature method (Du and Zhuo, 2009; Mara and Krömker, 2017), the OptD method (Błaszczak-Bąk et al., 2022), the neighbourhoods methods (Lubis et al., 2020), and a method based on the transformation of point clouds to regular voxels (Maturana and Scherer, 2015; Wu et al., 2015). The random method performs a random dataset reduction, and in the space method, the user sets a minimal distance between two points. Other methods generally reduce the point clouds on the flat surfaces while preserving the points on the differentiated surfaces. These approaches significantly reduce the datasets and do not result in a loss of important information.

Stage 3 (post-processing of the datasets) concerns the general 3D modelling of a monument. This stage is the most complex and

depends on many factors such as the available software used, the modelling approaches used, the complexity of the development, etc. The main tasks to be performed are the 3D reconstruction of the monument, RGB texturing, optimization of the 3D model, and preparation of the 3D visualization. The authors encourage the use of free software, such as CloudCompare, Blender, Meshroom, MeshLab, and many others. Each software has different capabilities, and it is often necessary to export and import models between them. The Poisson surface reconstruction method is frequently used for 3D modelling and triangular mesh generation. RGB texturing of the 3D model allows for a realistic visualization on the computer screen, closely resembling reality. It should be noted that TLS technology acquires large datasets, providing detailed information about sculptures but also potentially causing data redundancy. Therefore, there is often a need to optimize the point cloud by down-sampling point clouds. Additionally, the final 3D model may become too complex for further processing and should be simplified.

Stage 4 (3D printing) concerns preparation of the 3D model for printing. The 3D printer enables the creation of a physical scale replica of a 3D model that has been previously produced by a computer. The existing types of commercial 3D printers differ not only in their technology and impression mode, but also in the type of materials they use and in their physical-chemical features (Montuori et al., 2020; Nezhadarya et al., 2020). Preparation of a model for 3D printing generally depends on the type of technology used by the 3D printer (Shahrubudin et al., 2019), the type of materials used (Jandyal et al., 2022), and the technical properties of the printer. Often there is a need to reduce the detail of the 3D model or divide it into several parts because the printer's range is too small.

In the results section, an example from the study is presented to reflect the above stage.

3 Results

The proposed methodology of 3D sculpture documentation by TLS technology was tested on a real object. The research object, located at Polonia Square in Koszalin, Poland was a sculpture called the Monument to the Polish Diaspora Bond with the Homeland, also called the Eagles' Nest (https://polska-org.pl, 2023). By sculptor Romuald Grodzki, the four-sided sandstone pillar that narrows downwards was unveiled on 21 July 1976. Each face of the column has three vertical parts featuring bas-reliefs. The height of the monument is 7.61 m, and the width of its base is 0.90×0.90 m.

In stage 1, measurements were made using the terrestrial laser scanner Z+F IMAGER 5016, using tripods for six targets. The measurements were taken from four TLS positions (four scans were acquired). The height of the TLS was set at about 2.2 m, which allowed the details of the monument to be recorded. At each TLS position, the measurements were performed twice: at high resolution for the entire scene (horizontal 360° and vertical 320°) and at ultra-high resolution, though only for the sculpture. The purpose of the first measurement at high resolution (a density of points of 6.3 mm per 10 m) was to obtain data for the subsequent registration of the point clouds using the targets and the plane-to-plane method. It should be noted that the point clouds that do not belong to the relief and are useless for modelling are used to register the point clouds in one coordinate system. The purpose of the second measurement was to obtain ultra-high resolution data only on the sculpture (a density of points of 1.6 mm per 10 m). Additionally, RGB data was acquired through the scanner's built-in digital camera. The effect of light on a sculpture, especially on a cloudy day, has a significant impact on the quality of the photos taken automatically by a scanner. The quality of these photos is not always sufficient for textures and visualizations. Therefore, a series of photos was taken with manual settings using a Sony DSC-H300 digital camera at the maximum available resolution (5152×3864).

A photo of the research object and the locations of the measurement stations (1 – 4) and targets (t1 – t6) are presented in Figure 2.

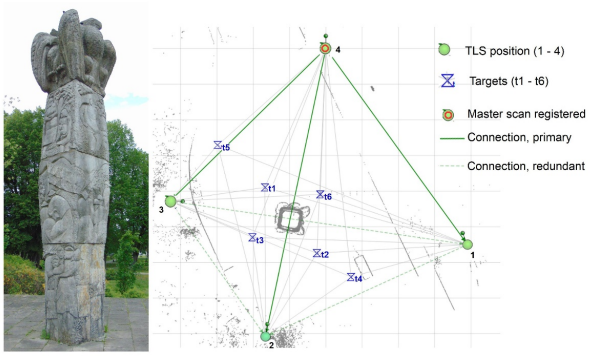

Figure 2. Research object (the Monument to the Polish Diaspora Bond with the Homeland) and measurement outline

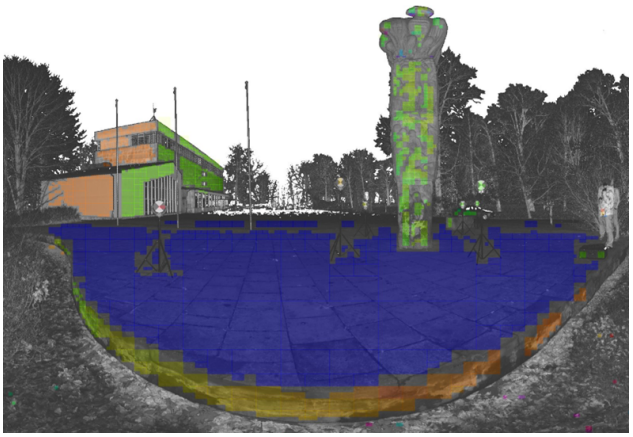

Figure 3. Fitting the planes into a point cloud

During stage 2, the pre-processing was completed using Z+F Laser-Control software. The RGB colouring of the point clouds and the data filtration from the noise were automatically performed. Next, the registration of the point clouds to one coordinate system was executed using a mixed approach (cloud-to-cloud, plane-to-plane, and targets). The choice of the point cloud registration approach depends on the given measuring equipment, the type of test object and the expected accuracy results. The process of registering data obtained by TLS technology has been well described in many publications (Cheng et al., 2018; Favre et al., 2021). Dataset registration is usually an automated process in a dedicated point cloud software. TLS position No. 4 was used as a reference block. Thus, the remaining point clouds were transformed to the local coordinate system defined at position No. 4. An example of fitting the planes into a point cloud is shown in Figure 3.

Table 1 summarizes the results of the point cloud registration. According to the statistics contained therein, the standard deviation for the fitting of each point cloud was 0.5 mm. The average registration error was also equal to 0.5 mm .

During the next step of stage 2, using CloudCompare 2.11.3 software, the point clouds were combined, and the monument was extracted. The point clouds captured from the neighbouring TLS stations were overlapped with each other, and thus, a down-sampling was needed. The space method was used to reduce the dataset by setting a minimum distance of 1 mm between two points. This allowed for the dataset to be reduced by 25% without a noticeable loss in quality.

In stage 3, the Poisson method (Kazhdan et al., 2020), implemented by the Poisson Surface Reconstruction plugin and using the octree structure, was used for the 3D reconstruction. The re-

Table 1. Adjusted translation parameters of the stations

No	Station	tx [m]	ty [m]	tz [m]	σ_X [m]	σ_Y [m]	σ_Z [m]	σ_{3D} [m]
1	Block_1	-12.253	-0.543	0.454	0.0003	0.0003	0.0003	0.0005
2	Block_2	-3.049	13.143	0.543	0.0003	0.0003	0.0003	0.0005
3	Block_3	-14.247	8.479	-0.444	0.0003	0.0003	0.0003	0.0005

Note: tx, ty, and tz are the offset vectors (shift vector of a given point cloud in relation to the reference point cloud); σ_X, σ_Y, and σ_Z the component standard deviations of the vectors; and σ_{3D} is standard deviation of the total fitting for $\sqrt{\sigma_X^2 + \sigma_Y^2 + \sigma_Z^2}$.

Figure 4. Visual comparison of 3D models of sculpture fragments for different octree depths (left – octree depth of 10, and right – octree depth of 11)

sult of such modelling is the generation of a triangular mesh. Once the 'normals' were created, the key element was to set the 'octree depth' parameter. The deeper the octree, the finer the result, but on the other hand, with a deeper octree, more time and memory are needed. Several tests were carried out to optimally set the 'octree depth' parameter. The study assumed an octree depth of 11 because of the sufficient resulting detail. It can be observed in Figure 4. Octree depth selection must be determined on a case-by-case basis.

The next step was the texturing of the 3D model. Texture generation can be completed in two ways. The first is to extract RGB information from photos taken with a digital camera during scanning. The second approach is to obtain RGB information from a series of photos taken manually with an external high-resolution digital camera. It should be noted that high-quality RGB data can significantly improve the realistic visualization of a 3D model on a computer screen. The second approach usually allows for much better-quality photos to be taken, which provides a more realistic texture effect but requires additional work. Therefore, it was decided to use the second approach of multi-image photogrammetry (Balletti et al., 2016; McCarthy, 2014). During the research, 273 photos were taken. Open-source Meshroom 2021.1.0 software was used to generate a textured model (Đurić et al., 2021). The distribution of the photos in relation to the sculpture is shown in Figure 5. The quality of the photos taken has a significant impact on the texturing of the resulting 3D model. Therefore, the lighting conditions of the scene should be taken into account during the tests. It is also recommended to use a colour checker for white balance in order to achieve natural photo colours.

The resulting model was saved as a set of files with the following extensions: *.obj (geometry data), *.mtl (material information), and five *.png files (textures). The model was imported to CloudCompare software. Two models were available in different coordinate systems: one built from point clouds (with high 3D accuracy) and the other created from a series of photos (with good RGB colour quality). This step of stage 3 is presented in Figure 6.

The models were registered to one coordinate system using initial fitting by common points and the 'fine registration' module. The reference model was the model created by the TLS point clouds. The RMS error was equal to 3.7 mm. Further texturing processes were completed using open-source Blender 3.4 software. The texture details were transferred from one model to the second using the Render Bake function in the Selected to Active mode. This function is commonly used in the creation of realistic textures based on the colour, lighting and shading information of a 3D model. In

Figure 5. Presentation of the position of the digital camera in relation to the sculpture in the Meshroom 2021.1.0 software

Figure 6. Two models in different coordinate systems (on the left a 3D model built from point cloud, on the right a 3D model built from a series of photos)

this way, the good attributes of both models were combined. The final 3D textured model in the blender window is shown in Figure 7. The 3D model contained 7 430 916 triangles, file size 1.1 GB, with resolution of the texture 8K (8192x8192 pix).

The resulting model is of good quality and high detail, but due to the very complex geometry (so-called high poly details), it could be difficult to use in real-time during a presentation. Therefore, the next step was to simplify the mesh by reducing the number of triangles and vertices while maintaining a compromise between the detail of the model and the desired performance (GharehTappeh and Peng, 2021). The preparation of models of lower detail (so-called low poly details) allows for the implementation of the level of detail (LOD) technique. The LOD technique is based on displaying models with various details, depending on factors such as the ob-

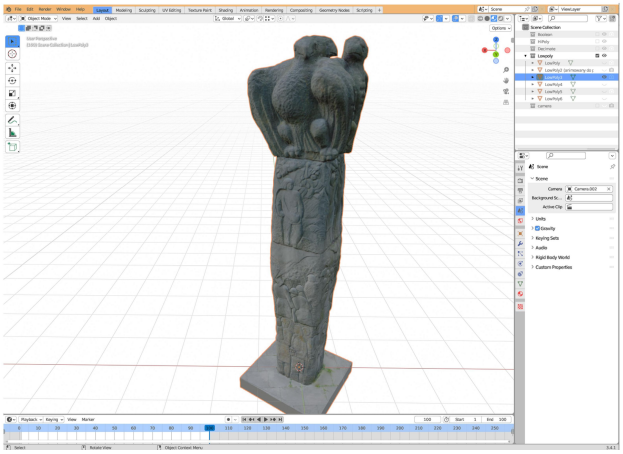

Figure 7. The final 3D textured model created using Blender software

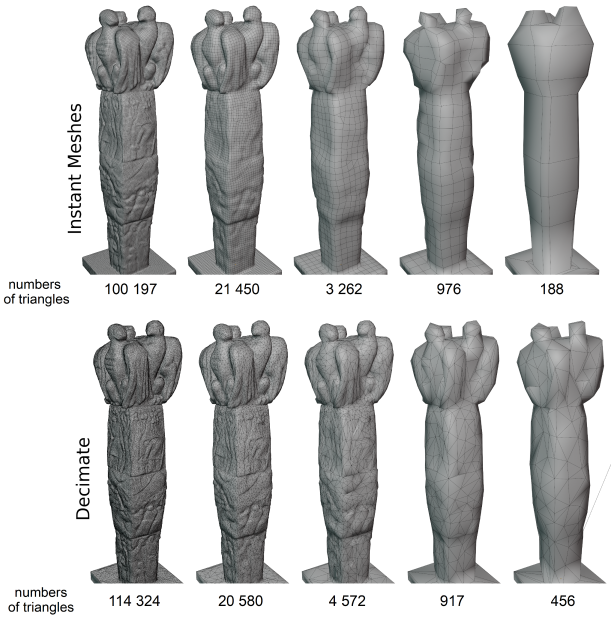

Figure 8. Comparison of the simplified models at different LOD levels (25.000%, 4.500%, 0.010%, 0.002%, and 0.001%)

ject's size, speed, and distance from the observer (Heok and Daman, 2004). Two methods were tested for the simplification of the 3D model: topology optimization using Instant Meshes software (Li et al., 2021) and simplification based on the modifier in Decimate software (Salwierz and Szymczyk, 2020). The reduction levels were manually set to 25.000%, 4.500%, 0.010%, 0.002%, and 0.001%. The simplified 3D models are presented and compared in Figure 8. The numbers of triangles are described below each model.

Based on a visual comparison of the obtained models, one can see that the mesh from the automatic retopology in Instant Meshes software was more regular, which allowed for easier work and editing. However, the Decimate modifier removed much more on the flat fragments and retained more detail in the more complex areas. The Decimate modifier is better for sculptures with very different areas and many details. Ultimately, a 25% reduced model was used for 3D printing. The detail of this model was sufficient for 3D printing.

During the last stage (stage 4), a modified Zonestar P802Q printer with a working area of 220×220×100 mm was used. The printer used fused deposition modelling technology (FDM). PLA material was used for printing. The height of the layers used for the two printed models was 0.2 mm. The working area of the printer

Figure 9. The 3D model (scale of 1:80)

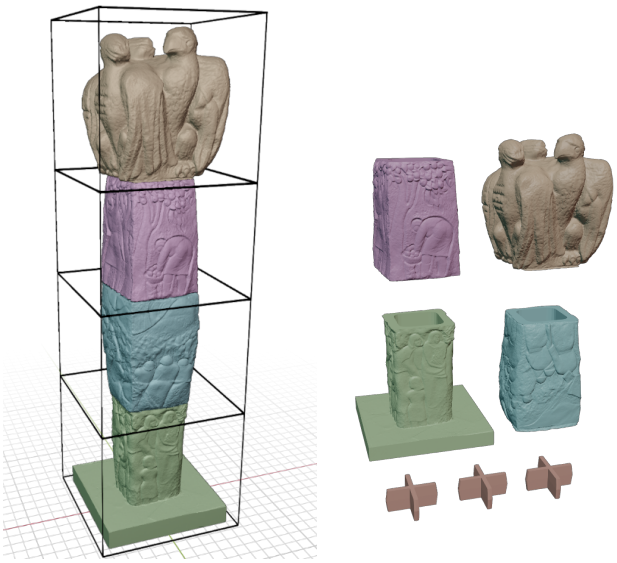

Figure 10. The division of the model into parts using Blender software

only allowed for printing the sculpture at a scale of 1:80 (Figure 9). Repetier-Host V2.2.4 was used to convert the object into specific instructions for the 3D printer. The final print was a general representation of the real object. The detail of the sculpture was significantly reduced compared to the 3D model due to the small size of the printed model and the limited resolution of the printer.

The figurine at a scale of 1:80 was not fully satisfactory, and so it was decided to print another one at a scale of 1:20, whose height, including the base, was 37.1 cm. This exceeded almost four times the vertical range of the printer. Thus, it was necessary to virtually divide the 3D model into four parts using Blender software. In order to reduce the amount of material used (and thus shorten the printing time) and facilitate the joining of the parts, holes were cut in the interior with a Boolean modifier (Salwierz and Szymczyk, 2020) and small connectors were prepared. The division of the model into parts to prepare for printing is presented in Figure 10. Next, the parts of the model were printed separately at a scale of 1:20.

The finished model of the sculpture was assembled by placing connectors between the parts of the monument, forcing the correct arrangement of the elements, and then gluing everything together. The final printed and merged 3D model is presented in Figure 11. The 1:20 scale model of the sculpture was characterized by sufficient detail and accurately reflected the real object.

It should be noted that the print quality of a 3D model also depends on the printer used. So, using a resin printer, for example, can improve the final detail of the 3D model sculpture when compared to a PLY printer.

Figure 11. The 3D model (scale of 1:20)

4 Discussion and Conclusions

The proposed process of preparing the 3D documentation of the monument in the form of a 3D printout of the model allowed for a faithful reconstruction of the sculpture at an adapted scale. TLS technology provided point clouds with sufficient resolution and accuracy. However, it was necessary to optimize the processes at each stage of processing due to the complex structure and detail of the object. This was mainly achieved by reducing the number of input points in stage 2, optimizing the 3D model in stage 3, and conducting fragmentary preparation of the printout in stage 4.

For stage 1 of the point cloud processing, Z+F LaserControl V9.2.2 (commercial software that was added to the laser scanner) and CloudCompare V2.12 alpha (free software) were used. All stages (stages 2–4) of the proposed methodology based on 3D modelling were performed using the free software, which should be considered an advantage. In this regard, of particular use was the capability offered by the Blender, Meshroom, and CloudCompare software, and their use made it possible to produce a very geometrically accurate and consistent 3D model.

The prepared 3D documentation of the Monument to the Polish Diaspora Bond with the Homeland in its 3D model printed form could be a valuable tool for a modelling operator to correctly reconstruct architectural details. Different LODs can be used for printing, depending on the purpose of the development, while the model preserved in the form of a digital record serve as the basis for the HBIM. The process of texturing the TLS model using an external RGB high-resolution digital camera is very good approach.

The Instant Mesh technique is a method that aims to automatically generate a simplified mesh with an optimized topology. It analyses the input model and produces a new mesh with reduced polygon count while preserving the overall shape and details as much as possible. An advantage of the Instant Mesh technique is a retention of shape and topology optimization and automation (because the process is automated, requiring minimal user input, making it convenient for quickly generating optimized meshes). Decimation, as implemented in software tools like Blender's Decimate modifier, involves reducing the polygon count of a 3D model by selectively removing vertices or triangles. The process allows for manual control over the level of simplification, as the user can adjust parameters to achieve the desired balance between complexity and quality. Advantages of the Decimate software technique are user control over the reduction process, and localized reduction (Decimation tools often include options for preserving important regions of the model while reducing complexity in less critical areas).

Based on our research the Decimate software technique provides more user control, allowing for manual adjustment of the simplification process and making it versatile for a range of 3D applications that require fine-tuning of complexity and performance trade-offs. It is recommended that less advanced users use the Instant Mesh technique. 3D models built with this technique are easier to process and view in real time on a computer screen.

The proposed methodology for the TLS point cloud processing for 3D modelling can be used in the following ways: (a) for a number of applications, such as 3D documentation, reconstruction, and education, and (b) for an efficient way to share information and knowledge about architectural heritage for professional users, societies, and experts involved in decision-making processes concerning such objects.

References

Al Khalil, O. (2020). Structure from motion (SfM) photogrammetry as alternative to laser scanning for 3D modelling of historical monuments. *Open Science Journal*, 5(2), doi:10.23954/osj.v5i2.2327.

Balletti, C., Beltrame, C., Costa, E., Guerra, F., and Vernier, P. (2016). 3D reconstruction of marble shipwreck cargoes based on underwater multi-image photogrammetry. *Digital Applications in Archaeology and Cultural Heritage*, 3(1):1–8, doi:10.1016/j.daach.2015.11.003.

Błaszczak-Bąk, W., Suchocki, C., and Mrówczyńska, M. (2022). Optimization of point clouds for 3D bas-relief modeling. *Automation in Construction*, 140:104352, doi:10.1016/j.autcon.2022.104352.

Bocheńska, A., Markiewicz, J., and Łapiński, S. (2019). The combination of the image and range-based 3D acquisition in archaeological and architectural research in the royal castle in Warsaw. *The International Archives of the Photogrammetry, Remote Sensing and Spatial Information Sciences*, 42(2/W15):177–184, doi:10.5194/isprs-archives-XLII-2-W15-177-2019.

Cheng, L., Chen, S., Liu, X., Xu, H., Wu, Y., Li, M., and Chen, Y. (2018). Registration of laser scanning point clouds: A review. *Sensors*, 18(5):1641, doi:10.3390/s18051641.

Du, X. and Zhuo, Y. (2009). A point cloud data reduction method based on curvature. In *2009 IEEE 10th International Conference on Computer-Aided Industrial Design & Conceptual Design*, pages 914–918. IEEE, doi:10.1109/CAIDCD.2009.5375038.

Favre, K., Pressigout, M., Marchand, E., and Morin, L. (2021). A plane-based approach for indoor point clouds registration. In *2020 25th International Conference on Pattern Recognition (ICPR)*, pages 7072–7079. IEEE, doi:10.1109/ICPR48806.2021.9412379.

GharehTappeh, Z. S. and Peng, Q. (2021). Simplification and unfolding of 3D mesh models: review and evaluation of existing tools. *Procedia CIRP*, 100:121–126, doi:10.1016/j.procir.2021.05.023.

Guidi, G. (2014). Terrestrial optical active sensors – theory & applications. In *3D recording and modelling in archaeology and cultural heritage: theory and best practices*, pages 39–62.

Heok, T. K. and Daman, D. (2004). A review on level of detail. In *International Conference on Computer Graphics, Imaging and Visualization, 2004, CGIV 2004*, pages 70–75. IEEE, doi:10.1109/CGIV.2004.1323963.

https://polska-org.pl (2023). Description of the monument. Retrieved from `https://polska-org.pl/8980295,Koszalin,Pomnik_Wiezi_Polonii_z_Macierza.html`. Last accessed April 2023.

Hui, Z., Cheng, P., Guan, Y., and Nie, Y. (2019). Review on airborne LiDAR point cloud filtering. *Laser & Optoelectronics Progress*, 55(6):060001, doi:10.3788/LOP55.060001.

Jandyal, A., Chaturvedi, I., Wazir, I., Raina, A., and Haq, M. I. U. (2022). 3D printing–a review of processes, materials and applications in industry 4.0. *Sustainable Operations and Computers*, 3:33–42, doi:10.1016/j.susoc.2021.09.004.

Kadhim, I., Abed, F. M., Vilbig, J. M., Sagan, V., and DeSilvey, C. (2023). Combining remote sensing approaches for detecting marks of archaeological and demolished constructions in Cahokia's Grand Plaza, Southwestern Illinois. *Remote Sensing*, 15(4):1057, doi:10.3390/rs15041057.

Kazhdan, M., Chuang, M., Rusinkiewicz, S., and Hoppe, H. (2020).

Poisson surface reconstruction with envelope constraints. In *Computer graphics forum*, volume 39, pages 173–182. Wiley Online Library, doi:10.1111/cgf.14077.

Klapa, P. and Gawronek, P. (2022). Synergy of geospatial data from TLS and UAV for Heritage Building Information Modeling (HBIM). *Remote Sensing*, 15(1):128, doi:10.3390/rs15010128.

Li, H., Yamada, T., Jolivet, P., Furuta, K., Kondoh, T., Izui, K., and Nishiwaki, S. (2021). Full-scale 3D structural topology optimization using adaptive mesh refinement based on the level-set method. *Finite Elements in Analysis and Design*, 194:103561, doi:10.1016/j.finel.2021.103561.

Lubis, A. R., Lubis, M., and Al, K. (2020). Optimization of distance formula in K-Nearest Neighbor method. *Bulletin of Electrical Engineering and Informatics*, 9(1):326–338, doi:10.11591/eei.v9i1.1464.

Mara, H. and Krömker, S. (2017). Visual computing for archaeological artifacts with integral invariant filters in 3D. In *GCH 2017 – Eurographics Workshop on Graphics and Cultural Heritage*, pages 37–47. doi:10.2312/gch.20171290.

Maturana, D. and Scherer, S. (2015). Voxnet: A 3D convolutional neural network for real-time object recognition. In *IEEE/RSJ International Conference on Intelligent Robots and Systems*. doi:10.1109/IROS.2015.7353481.

McCarthy, J. (2014). Multi-image photogrammetry as a practical tool for cultural heritage survey and community engagement. *Journal of Archaeological Science*, 43:175–185, doi:10.1016/j.jas.2014.01.010.

Mistretta, F., Sanna, G., Stochino, F., and Vacca, G. (2019). Structure from motion point clouds for structural monitoring. *Remote Sensing*, 11(16):1940, doi:10.3390/rs11161940.

Montuori, R., Gilabert-Sansalvador, L., and Rosado-Torres, A. L. (2020). 3D printing for dissemination of Maya architectural heritage: The Acropolis of La Blanca (Guatemala). *The International Archives of the Photogrammetry, Remote Sensing and Spatial Information Sciences*, 44(M-1):481–488, doi:10.5194/isprs-archives-XLIV-M-1-2020-481-2020.

Murtiyoso, A., Grussenmeyer, P., Landes, T., and Macher, H. (2021). First assessments into the use of commercial-grade solid state lidar for low cost heritage documentation. *The International Archives of the Photogrammetry, Remote Sensing and Spatial Information Sciences*, 43(B2):599–604, doi:10.5194/isprs-archives-XLIII-B2-2021-599-2021.

Neumüller, M., Reichinger, A., Rist, F., and Kern, C. (2014). 3D printing for cultural heritage: Preservation, accessibility, research and education. In *Lecture Notes in Computer Science (Including Subseries Lecture Notes in Artificial Intelligence and Lecture Notes in Bioinformatics)*, volume 8355, pages 119–134. Springer, doi:10.1007/978-3-662-44630-0_9.

Nezhadarya, E., Taghavi, E., Razani, R., Liu, B., and Luo, J. (2020). Adaptive hierarchical down-sampling for point cloud classification. In *Proceedings of the IEEE/CVF Conference on Computer Vision and Pattern Recognition*, pages 12956–12964. doi:10.1109/CVPR42600.2020.01297.

Nowak, R., Orłowicz, R., and Rutkowski, R. (2020). Use of TLS (LiDAR) for building diagnostics with the example of a historic building in Karlino. *Buildings*, 10(2):24, doi:10.3390/buildings10020024.

Rodríguez-Gonzálvez, P., Jimenez Fernandez-Palacios, B., Muñoz-Nieto, Á. L., Arias-Sanchez, P., and Gonzalez-Aguilera, D. (2017). Mobile LiDAR system: New possibilities for the documentation and dissemination of large cultural heritage sites. *Remote Sensing*, 9(3):189, doi:10.3390/rs9030189.

Salwierz, A. and Szymczyk, T. (2020). Methods of creating realistic spaces–3D scanning and 3D modelling. *Journal of Computer Sciences Institute*, 14:101–108, doi:10.35784/jcsi.1584.

Sammartano, G., Avena, M., Fillia, E., and Spanò, A. (2023). Integrated HBIM-GIS models for multi-scale seismic vulnerability assessment of historical buildings. *Remote Sensing*, 15(3):833, doi:10.3390/rs15030833.

Shahrubudin, N., Lee, T. C., and Ramlan, R. (2019). An overview on 3D printing technology: Technological, materials, and applications. *Procedia Manufacturing*, 35:1286–1296, doi:10.1016/j.promfg.2019.06.089.

Shih, N.-J. and Chen, Y. (2020). LiDAR-and AR-Based monitoring of evolved building facades upon zoning conflicts. *Sensors*, 20(19):5628, doi:10.3390/s20195628.

Suchocki, C., Błaszczak-Bąk, W., Damięcka-Suchocka, M., Jagoda, M., and Masiero, A. (2020a). On the use of the OptD method for building diagnostics. *Remote Sensing*, 12(11):1806, doi:10.3390/rs12111806.

Suchocki, C., Błaszczak-Bąk, W., Janicka, J., and Dumalski, A. (2021). Detection of defects in building walls using modified OptD method for down-sampling of point clouds. *Building Research & Information*, 49(2):197–215, doi:10.1080/09613218.2020.1729687.

Suchocki, C., Damięcka-Suchocka, M., Katzer, J., Janicka, J., Rapiński, J., and Stałowska, P. (2020b). Remote detection of moisture and bio-deterioration of building walls by time-of-flight and phase-shift terrestrial laser scanners. *Remote Sensing*, 12(11):1708, doi:10.3390/rs12111708.

Tan, K., Cheng, X., Ju, Q., and Wu, S. (2016). Correction of mobile TLS intensity data for water leakage spots detection in metro tunnels. *IEEE geoscience and remote sensing letters*, 13(11):1711–1715, doi:10.1109/LGRS.2016.2605158.

Temizer, T., Nemli, G., Ekizce, E., Ekizce, A., Demir, S., Bayram, B., Askin, F., Cobanoglu, A., and Yilmaz, H. (2013). 3D documentation of a historical monument using terrestrial laser scanning case study: Byzantine Water Cistern, Istanbul. *The International Archives of the Photogrammetry, Remote Sensing and Spatial Information Sciences*, 40:623–628, doi:10.5194/isprsarchives-XL-5-W2-623-2013.

Teppati Losè, L., Spreafico, A., Chiabrando, F., and Giulio Tonolo, F. (2022). Apple LiDAR sensor for 3D surveying: Tests and results in the cultural heritage domain. *Remote Sensing*, 14(17):4157, doi:10.3390/rs14174157.

Đurić, I., Vasiljević, I., Obradović, M., Stojaković, V., Kićanović, J., and Obradović, R. (2021). Comparative analysis of open-source and commercial photogrammetry software for cultural heritage. In *eCAADe 2021 International Scientific Conference*, pages 8–10. doi:10.52842/conf.ecaade.2021.2.243.

Wabiński, J. and Mościcka, A. (2019). Natural heritage reconstruction using full-color 3D printing: a case study of the valley of five Polish ponds. *Sustainability*, 11(21):5907, doi:10.3390/su11215907.

Wu, Z., Song, S., Khosla, A., Yu, F., Zhang, L., Tang, X., and Xiao, J. (2015). 3d shapenets: A deep representation for volumetric shapes. In *Proceedings of the IEEE conference on computer vision and pattern recognition*, pages 1912–1920. doi:10.1109/CVPR.2015.7298801.

Xu, Z., Wu, L., Shen, Y., Li, F., Wang, Q., and Wang, R. (2014). Tridimensional reconstruction applied to cultural heritage with the use of camera-equipped UAV and terrestrial laser scanner. *Remote sensing*, 6(11):10413–10434, doi:10.3390/rs61110413.

Yan, W., Behera, A., and Rajan, P. (2010). Recording and documenting the chromatic information of architectural heritage. *Journal of cultural heritage*, 11(4):438–451, doi:10.1016/j.culher.2010.02.005.

Youn, H.-C., Yoon, J.-S., and Ryoo, S.-L. (2021). HBIM for the characteristics of Korean traditional wooden architecture: bracket set modelling based on 3d scanning. *Buildings*, 11(11):506, doi:10.3390/buildings11110506.

Zheng, J., Zhang, J., Li, J., Tang, R., Gao, S., and Zhou, Z. (2020). Structured3d: A large photo-realistic dataset for structured 3d modeling. In *Computer Vision–ECCV 2020: 16th European Conference, Glasgow, UK, August 23–28, 2020, Proceedings, Part IX 16*, pages 519–535. Springer, doi:10.1007/978-3-030-58545-7_30.

Appendix A

Technical characteristics of the terrestrial laser scanner and additional equipment:

The terrestrial laser scanner Z+F IMAGE 5016, telescope tripod with 3D safety adapter, six Z+F targets with special tripod were used to the research. During the measurement, the instrument was controlled using a Microsoft Surface Pro 6 tablet. The equipment was presented in the photography.

The technical parameters Z+F Imager 5016 scanner

Laser class	1
Type of rangefinder	Phase-Shift
Type of wavelength	Infrared
Measurement range	0.3 – 365 m
Range resolution	0.1 mm
Linearity error	±1 mm + 10 ppm/m
Data acquisition rate	Max. 1.1 million pixel/sec.
Beam diameter/ divergence	~ 3.5 mm @ 1m / ~ 0.3 mrad ($1/e^2$, half angle)
Angular resolution, vertically / horizontally	0.00026° (0.93 arcsec) / 0.00018° (0.65 arcsec
Vertical / Horizontal accuracy	0.004° (14.4 arcsec) rms / 0.004° (14.4 arcsec) rms
Operating temperature / Storage temperature	-10 °C … +45 °C / -20 °C … +50 °C
Field of view (h/v)	360° / 320°
Additional sensors	HDR camera, positioning system (barometer, acceleration sensor, gyroscope, compass, GPS)
Ethernet link	1 GB Ethernet
Data storage	128 GB SATA
Integrated control panel	5.7” touch screen
Scanner dimensions (w×d×h)	150×258×328 mm
Scanner weight	6.5 kg